Investigation of formation of secondary pollutant (ozone) in the atmosphere of Tomsk

D.A. Belikov and A.V. Starchenko

Institute of Atmospheric Optics,
Siberian Branch of the Russian Academy of Sciences, Tomsk

Received January 24, 2005

To monitor and study of the urban air pollution by troposphere ozone, prognostic models of spreading pollution taking unto account schemes of secondary pollutant formation are proposed. Eulerian model of turbulent diffusion containing transport equation with description of advection, turbulent diffusion, and chemical reactions is used. In this work, three reduced kinetic mechanisms of secondary pollutant formation are approved and compared with observed data. A short-term forecast the urban weather is realized with the use of an one-dimensional unsteady model of atmospheric boundary layer. The following sources of primary pollution are considered: industrial and heat power stacks (point sources), vehicle emissions (linear sources), and large industrial area (area sources). The mathematical problem is solved with use of a finite volume method. One of the proposed models was applied to reveal the features of the urban air pollution by ozone and its precursors, to determine factors of pollution generation and destruction, to analyze the dynamics of diurnal ozone distribution for various seasons. Results of comparison of predictions and observations allow one to apply used models, which main advantage is high performance in forecasting of secondary air pollution distribution above urban regions.

Introduction

Processes in the low atmosphere (boundary layer) significantly affect human life and activity.[1] Even little changes in moisture exchange between the ground surface and atmosphere, radiation balance, chemical composition of air and other characteristics have serious consequences for environment. That is why simulation of atmospheric processes is now the issue of the day for monitoring and forecast of ecological and meteorological state of the atmospheric boundary layer. It is especially important in the period of rapid development of industry, power engineering, and vehicles, when the atmospheric air deteriorates constantly due to increase in the number of factors affecting its chemical and aerosol composition.

In the past decades, simulation models are widely used for scenario computations designed to clarify specific features of pollution propagation over some chosen area under different weather conditions.[2] The scenario analysis is carried out to study the contribution of a separate source to air pollution,[3] as well as to estimate effects of possible emergency situations at extra-hazardous objects.[4] Moreover, simulation models are included in on-line systems of air quality monitoring. Such systems provide for a real-time detailed information on distribution of pollution concentration in air over urban territories uncovered with stationary observation sites, using data of high certainty from measurement sites.[5,6]

The analysis of the air pollution state can not be complete without taking into account the contribution of secondary emission products, i.e., resultants of chemical and photochemical reactions between constituents of man-made emission and air. Many of such compounds are highly toxic; they form so-called urban photochemical smog, which lowers the visibility and affects detrimentally human beings, animals and plants.[7]

Models of impurity transport with integrated blocks (procedures) of chemical reactions based on chemical kinetics equations are used to calculate concentrations of secondary pollutants. Today many models are designed to estimate concentrations of secondary pollutants with a precision depending in many respects on the number of considering constituents and connecting equations, varying from tens to few hundreds in different procedures (Refs. 2, 8–12).

The purpose of this paper is to compare three abridged kinetic models of ozone generation and to study possibilities of their use for investigation of formation of secondary pollutants in Tomsk city and its suburbs. We intend to reveal peculiarities of urban air pollution with ozone, to determine the factors affecting formation and destruction of secondary pollutants, and to study their diurnal behavior in different seasons.

Impurity transport model considering chemical interactions

The Euler turbulent diffusion model is applied by us to calculate the concentration of interacting impurity components. The model includes transport equations describing advection, turbulent diffusion, and chemical reactions[13]:

0235-6880/05/05–06 391-08 $02.00

$$\frac{\partial C_i}{\partial t} + U\frac{\partial C_i}{\partial x} + V\frac{\partial C_i}{\partial y} + W\frac{\partial C_i}{\partial z} = \\ = -\frac{\partial}{\partial x}\langle c_i u\rangle - \frac{\partial}{\partial y}\langle c_i v\rangle - \frac{\partial}{\partial z}\langle c_i w\rangle + S_i + R_i, \quad i = 1, \ldots, n, \tag{1}$$

where $C_i(t, x, y, z)$ is the concentration of ith component of impurity; S_i is the source term representing emission of impurity components to atmosphere and their deposition on the underlying surface; R_i describes formation of a substance due to chemical reactions with participation of impurity components; t is time; x, y, and z are spatial coordinates. Capital letters denote averaged terms, small letters denote pulsating terms, angular brackets denote time averaging.

The technique of computation of wind velocity components U, V, and W, and turbulent correlations of concentration with the wind velocity components $\langle c_i u\rangle, \langle c_i v\rangle, \langle c_i w\rangle$ from Eq. (1), as well as applied models of the atmospheric boundary layer and turbulence are described in detail in Ref. 14.

The modeling of gas-phase photochemistry is carried out on the base of three simplified models: the Azzi semiempirical kinetic model used in the Hurley model,[9] the AIRCHEM photochemical module,[10] and the abridged kinetic mechanism RADM.[11]

The Azzi model is based on the semiempirical mechanism GRS (Generic Reaction Set) containing 11 chemical components (smog-producing reactivity R_{smog}, organic radicals RP, H_2O_2, NO, NO_2, O_3, SO_2, stable non-gaseous organic carbon products SNGOC, stable gaseous nitrogen products SGN, stable non-gaseous nitrogen products SNGN, stable non-gaseous nitrogen sulfur products SNGS) participating in 8 chemical reactions (Table 1). This model, complemented with water-phase reactions for sulfur dioxide and aerosols, is included into three-dimensional non-hydrostatic model TAMP (The Air Pollution Model)[9] with vertical coordinate accounting for the relief. The TAMP is the program system aimed at the study of mesoscale meteorology, as well as the transport and transformation of pollutants. To present the impurity dispersion near some point source more accurately, the Lagrangian Particle Module is applied; the buoyancy effect is considered by the Plum Rise Model; the Eulerian Grid Model solves the prognostic transport equation accounting for effects of wet and dry deposition.

Table 1. Reactions and rate of reactions of the Azzi photochemical model

Reaction	Reaction rate
$R_{smog} + h\nu \rightarrow RP + R_{smog} + \eta$SNGOC	$R_1 = k_1 C_{Rsmog}$
$RP + NO \rightarrow NO_2$	$R_2 = k_2 C_{RP} C_{NO}$
$NO_2 + h\nu \rightarrow NO + O_3$	$R_3 = k_3 C_{NO_2}$
$NO + O_3 \rightarrow NO_2$	$R_4 = k_4 C_{NO} C_{O_3}$
$RP + RP \rightarrow RP + \alpha H_2O_2$	$R_5 = k_5 C_{RP} C_{RP}$
$RP + NO_2 \rightarrow$ SGN	$R_6 = k_6 C_{RP} C_{NO_2}$
$RP + NO_2 \rightarrow$ SNGN	$R_7 = k_7 C_{RP} C_{NO_2}$
$RP + SO_2 \rightarrow$ SNGN	$R_8 = k_8 C_{RP} C_{SO_2}$

AIRCHEM module[10] is a block of chemical reactions of the duplex HIRES-AIRCHEM system used to investigate both local and regional problems of secondary pollutants. The version in use includes 10 components (O_3, NO, NO_2, aldehydes ALD, OH, RO_2 hydrocarbon radicals, CH hydrocarbon products, HO_2, CO, O) participating in 10 reactions (Table 2).

Table 2. Reactions and rate of reactions of the AIRCHEM photochemical module

Reaction	Reaction rate
$RH + OH \rightarrow 4RO_2 + 2ALD$	$R_1 = k_1 C_{RH} C_{OH}$
$ALD + h\nu \rightarrow 2HO_2 + CO$	$R_2 = k_2 C_{ALD}$
$RO_2 + NO \rightarrow NO_2 + ALD + HO_2$	$R_3 = k_3 C_{RO_2} C_{NO}$
$HO_2 + NO \rightarrow NO_2 + OH$	$R_4 = k_4 C_{HO_2} C_{NO}$
$NO_2 + h\nu \rightarrow NO + O_3$	$R_5 = k_5 C_{NO_2}$
$NO + O_3 \rightarrow NO_2 + O_2$	$R_6 = k_6 C_{NO} C_{O_3}$
$O_3 + h\nu \rightarrow O_2 + O(^1D)$	$R_7 = k_7 C_{O_3}$
$O(^1D) + H_2O \rightarrow 2OH$	$R_8 = k_8 C_{O(^1D)} C_{H_2O}$
$NO_2 + OH \rightarrow HNO_3$	$R_9 = k_9 C_{NO_2} C_{OH}$
$CO + OH \rightarrow CO_2 + HO_2$	$R_{10} = k_{10} C_{CO} C_{OH}$

Three problems of different scales were investigated[10] with the HIRES-AIRCHEM. The first was a local problem of ozone pollution of the Sidney air basin. The second combined local and regional problems of passage of a forest fire plume, distant from Sidney to more then 10 km, through the Sidney atmosphere. The third was a problem of long-distant transport in south-east Asia of Indonesian forest fire smoke.

The abridged kinetic mechanism RADM (Ref. 11) includes 11 components (O_3, NO, NO_2, O, RH hydrocarbon products, OH, RO_2 hydrocarbon radicals, aldehydes RCHO, anions of organic acids $RC(O)O_2$, HO_2, paracetylnitrate (PAN) $RC(O)O_2NO_2$) interacting with each other in 12 reactions (Table 3).

The impurity transport simulation model,[11] including the processes of diffusion and advection, dry deposition, and chemical reactions of kinetic mechanism RADM, was used to study the spatiotemporal distribution of near-ground ozone concentrations depending on the emission mode and weather conditions, as well as for analysis of air pollution in San-Huan (Argentina).

Table 3. Reactions and rate of reactions of the photochemical model of the abridged kinetic mechanism RADM

Reaction	Reaction rate
$NO_2 + h\nu \rightarrow NO + O$	$R_1 = k_1 C_{NO_2}$
$O + O_2 \rightarrow O_3$	$R_2 = k_2 C_O$
$NO + O_3 \rightarrow NO_2$	$R_3 = k_3 C_{NO} C_{O_3}$
$RH + OH \rightarrow RO_2$	$R_4 = k_4 C_{RH} C_{OH}$
$RCHO + OH \rightarrow RC(O)O_2$	$R_5 = k_5 C_{RCHO} C_{OH}$
$RCHO + h\nu \rightarrow RO_2 + HO_2$	$R_6 = k_6 C_{RCHO}$
$NO + HO_2 \rightarrow NO_2 + OH$	$R_7 = k_7 C_{NO} C_{HO_2}$
$RO_2 + NO \rightarrow NO_2 + HO_2 + RCHO$	$R_8 = k_8 C_{RO_2} C_{NO}$
$RC(O)O_2 + NO \rightarrow NO_2 + RO_2$	$R_9 = k_9 C_{RCOO_2} C_{NO}$
$NO_2 + OH \rightarrow NO + H_2O$	$R_{10} = k_{10} C_{NO_2} C_{OH}$
$RC(O)O_2 + NO_2 \rightarrow RC(O)O_2NO_2$	$R_{11} = k_{11} C_{RCOO_2} C_{NO_2}$
$RC(O)O_2NO_2 \rightarrow RC(O)O_2 + NO_2$	$R_{12} = k_{12} C_{RCOO_2NO_2}$

The list of components used in the Azzi kinetic model and the abridged kinetic mechanism RADM was supplemented with the carbon monoxide considered as a chemically resistant component in these kinetic models. This addition was made, because the chosen simulation models of impurity transport and transformation were tested on the base of data of the TOR Station IAO SB RAS, which measures routinely only few small constituents of the atmospheric ground layer, including carbon monoxide. Therefore, this component can be treated as a criterion of adequacy of representation of some numerical model of impurity transfer through advection and turbulent diffusion.

Initial and boundary conditions

The background concentrations, preliminarily calculated at each step by the box model (at a single cell) on the base of chemical reactions only (without accounting for transport and turbulent diffusion), are used as boundary conditions at input side boundaries. Initial background values for ozone, nitric oxide and dioxide were chosen from the measurement data of the TOR Station.

As the measurements were carried out in the east outskirts of Tomsk (Fig. 1), the nighttime concentrations of O_3, NO, and NO_2 measured at wind directions from north-east to south-east were taken as the initial background values, because the filling flow arrived from the unpolluted territories. Background values of hydrocarbons were taken equal to 0.2 ppb; zero initial and background values were taken for other components because of the absence of measurement data.

When initializing the model, concentrations of the considered impurity components were taken equal to initial background values all over the domain of calculations.

Ordinary gradient constrains were placed on the upper boundary. Conditions simulating dry deposition of impurity components were used for the bottom boundary[15]:

$$-\langle c_i w\rangle = vd_i C_i, \qquad (2)$$

$$vd_i = \frac{1}{r_a + r_b + r_c}, \quad r_a = \frac{\Psi(z/z_{0t}, z/L)}{\kappa u_*},$$

$$r_b = \frac{2(\mathrm{Sc}_i/0.72)^{\frac{2}{3}}}{\kappa u_*}, \quad r_c = 60.0 \text{ s/m};$$

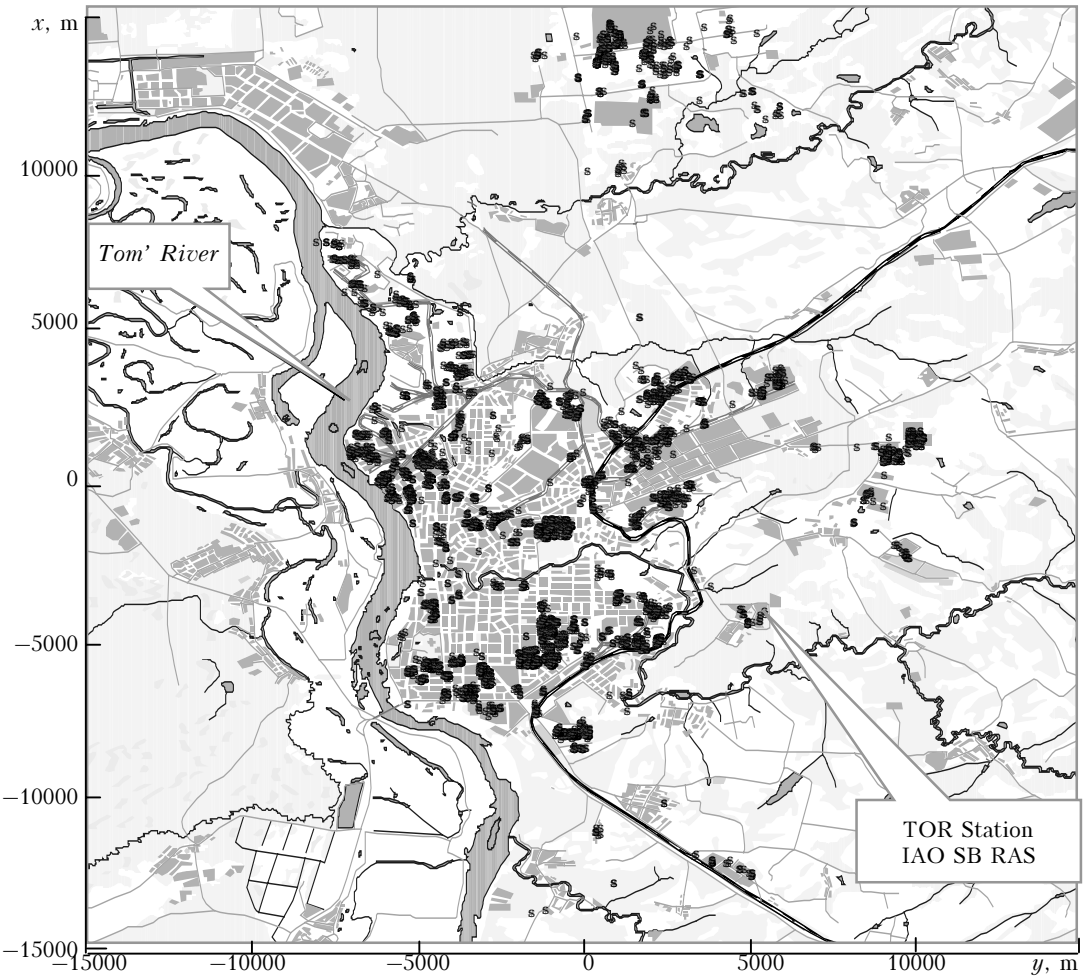

Fig. 1. Region of investigation and distribution of stationary air pollution sources (marked in black) in Tomsk and its outskirts.

$$\Psi(z/z_{0t}, z/L) = \begin{cases} \ln(z_{0t}/L) - 2\ln\left(\dfrac{1+\sqrt{1-9\,z/z_{0t}}}{1+\sqrt{1-9\,z/L}}\right), & z/L \le 0, \\ \ln(z/z_{0t}) + 6.34\left(\dfrac{z}{L} - \dfrac{z_{0t}}{L}\right), & z/L > 0, \end{cases}$$

where vd_i is the deposition rate of ith component of impurity; r_a is the aerodynamic drag of the turbulent atmosphere; r_b is the surface resistance of roughness elements; r_c is the resistance due to vegetation; z is the height; z_{0t} is the thermal height of roughness; L is the Obukhov scale; Sc_i is the Schmidt number for ith component of impurity; $\kappa = 0.40$ is the Karman constant; u_* is the friction velocity.

Computation technique

The spatial unsteady equations (1) have been solved numerically for a parallelepiped with numerous surface and high-altitude sources. To calculate the impurity transport, it is necessary to compute fields of temperature, humidity, wind speed and direction with the use of the atmospheric boundary layer model.[14]

Differential operators in Eqs. (1) were approximated with the second order of accuracy in coordinates and the first order of accuracy in time, using explicit difference schemes for all terms of the equation except for the vertical diffusion.

Such method of discretization of the differential problem allowed us to solve problems arising from nonlinearity of Eqs. (1) and to accelerate significantly the solution obtaining due to the use of the efficient sweep method with acceptable restriction of the time step. The advective terms of transport equations (1) were approximated using the monotonic upstream Van Leer scheme, which does not allow non-physical concentration values to appear.

Accounting for chemical reactions resulting in formation of the secondary pollutants increases significantly the computation time, therefore high-performance computers were used, in particular, multiprocessor cluster systems of the Institute of Atmospheric Optics SB RAS (http://cluster.iao.ru) and the Tomsk State University (http://cluster.tsu.ru) with the MPI (Message Passing Interface) installed.

The numerical solution of Eqs. (1) was paralleled using the geometric principle of data decomposition. The entire domain of investigation was divided into identical regions. In this study, the domain's parallelepiped ($-L_x/2 \le x \le L_x/2$; $-L_y/2 \le y \le L_y/2$; $0 \le z \le L_{iz}$) was cut into sections $y = \text{const}$ and the data from each region were assigned to the corresponding processor element. All grid concentration values $(c_j)^{n+1}_{k,l,m}$ were uniformly distributed over the computational nodes of the distributed-memory multiprocessor system.

Inside every region, the grid equations obtained from discretization of Eqs. (1) were solved simultaneously by the sweep method. However, because of the selected difference mask, two grid values of the concentration from the neighboring region were needed when calculating the concentrations along the near-boundary grid line. Therefore, for correct operation of the parallel program, it was necessary to organize the exchange of near-boundary grid values between the processors. This task was solved using the MPI_SendRecv library function. Besides, for preparation of parallel computations, the following Message Passing Interface library functions were invoked: MPI_Bcast and MPI_Scatter.

Computational conditions and discussion of results

The presented models of transport and chemical transformation of impurities were applied to analyze the polluting of Tomsk air with secondary emission products in different seasons. A special attention was focused on formation of near-ground ozone as one of the most common secondary pollutant and extremely dangerous matter. To estimate a certainty of results, the observational data on changes of meteorological parameters (air temperature and humidity, solar radiation, wind direction and speed) were used, as well as concentrations of ozone, nitric oxide and dioxide measured at the TOR Station (Fig. 1).

The calculations were performed in the parallelepiped domain of 2 km in height, 30×30 km in foundation with Tomsk at the center (Fig. 1). In the domain, we have built a $100 \times 100 \times 50$ grid, uniform horizontally, non-uniform vertically and becoming denser in the direction to the surface. In the calculations, 119 linear sources, 12 area sources, and 338 point ones were considered. Intensity of vehicular impurity intake was assumed to change daily according to Fig. 2 (Ref. 16). Total volume of nitric oxides in vehicles air pollution included 75% of nitric monoxide and 25% of dioxide.[16]

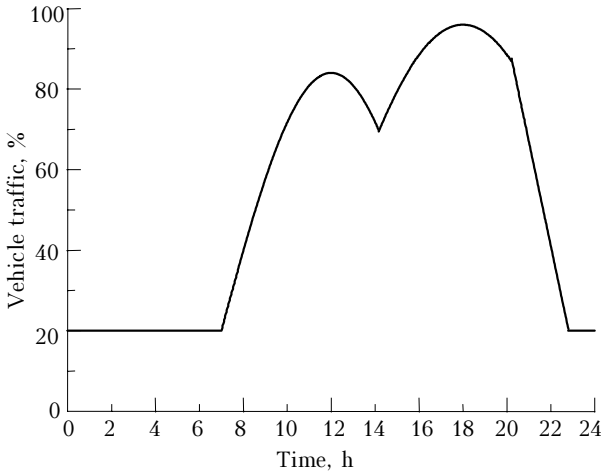

Fig. 2. Time dependence of vehicle traffic.[16]

Figure 3 shows the calculation data and the data measured at the TOR Station operation zone on

February 19–20, 2004. Calculated profiles show the ground level ozone concentration to increase after the sunrise up to its peak in the afternoon, when the peak of solar activity is over.

This is caused by a significant role of the photochemical reaction of NO_2 photolysis during daylight hours, when its rate is higher than the rate of the reverse reaction $O_3 + NO \rightarrow NO_2 + O_2$. Such a situation leads to nitric dioxide reduction, since its emission level is not high in suburbs.

Note, that in the described kinetic models, in parallel with the reaction of NO_2 photolysis with two resultant reactive species (NO and O), we consider photochemical decomposition reactions of volatile compounds of man-made emission with formation of radicals, which, reacting with NO, result in appearance of nitric dioxide. In our case (see Fig. 3), the wind direction was such that the domain of measurements and calculations fell into the windward part of suburbs, where urban sources contributed insignificantly to the air pollution.

The nighttime is characterized by the absence of photochemical reactions, therefore NO oxidizes to NO_2 with O_3 consumption. Thus, diurnal variations of ground level concentrations are similar for nitric oxide and ozone.

Calculated ground level concentrations of impurity components and meteorological parameters as well as observational data for October 15–16, 2003, shown in Fig. 4, are qualitatively similar to results obtained for February 19–20, 2004.

The ground level concentrations of ozone and NO_2 are higher as compared to those in Fig. 3 at close values of solar radiation, which is stipulated, first of all, by the west and southwest (220–280°) winds in the observation period, transporting urban pollutants to the TOR Station. Of great concern in this case is the generation of the "secondary" nitric dioxide as a result of chemical reaction of radicals with nitric monoxide (NO concentration lowering in Fig. 4 as compared to Fig. 3), photolysis of which favors the increase of the ground level ozone concentration. Besides, augmentation of ozone is caused by a lower speed of the surface wind on October 15–16, 2003 in comparison with February 19–20, 2004 (Figs. 3 and 4).

Figure 5 gives a comparison of calculations performed by the chosen abridged kinetic models and observed on May 26–27, 2004.

A good correspondence between the predicted and measured ground level concentrations of ozone, nitric dioxide, carbon monoxide, and meteorological parameters is obvious. Since the solar radiation level in this case is higher then in the observation periods described above, both the calculations and measurements give higher ozone concentrations in the daytime.

An explicit radiation dependence of other trace components is seen as well: hydroxyl group (OH), peroxide group (HO_2), and hydrocarbon radicals, caused by photochemical decomposition reaction of volatile constituents of vehicles and industrial emissions.

Distinctive night maxima and day minima of the carbon monoxide concentration (Fig. 5) are caused obviously by the locking inversion factor. The radiative surface cooling decreases the turbulent exchange in the ground layer and, correspondingly,

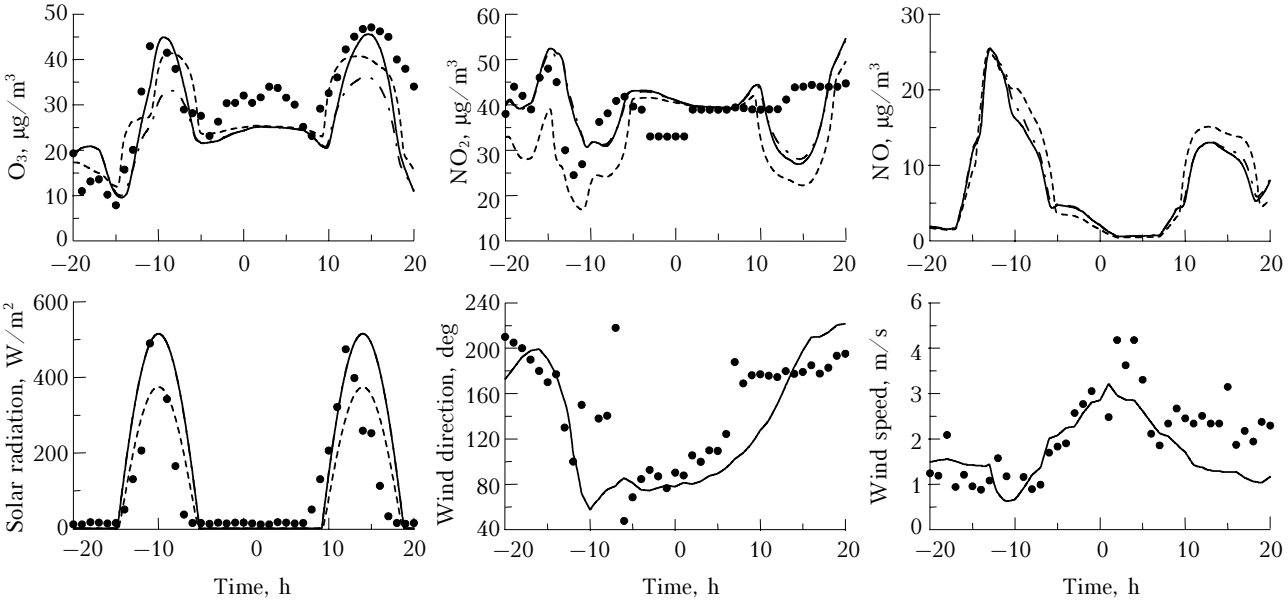

Fig. 3. Comparison of ozone, nitric oxide and dioxide concentrations; wind speed and direction; solar radiation (February 19–20, 2004), calculated by different models and measured. The negative part of axis corresponds to the first day of modeling, positive one – to the second day. Symbols represent the measured data and curves – calculated ones: the abridged mechanism RADM (solid curves), the AIRCHEM mechanism (dashed curves), the GRS model (dotted lines). The following initial background values were used in calculations: 29 μg/m^3 (O_3), 28 μg/m^3 (NO_2), 4.3 μg/m^3 (NO), and 0.1 mg/m^3 (CO).

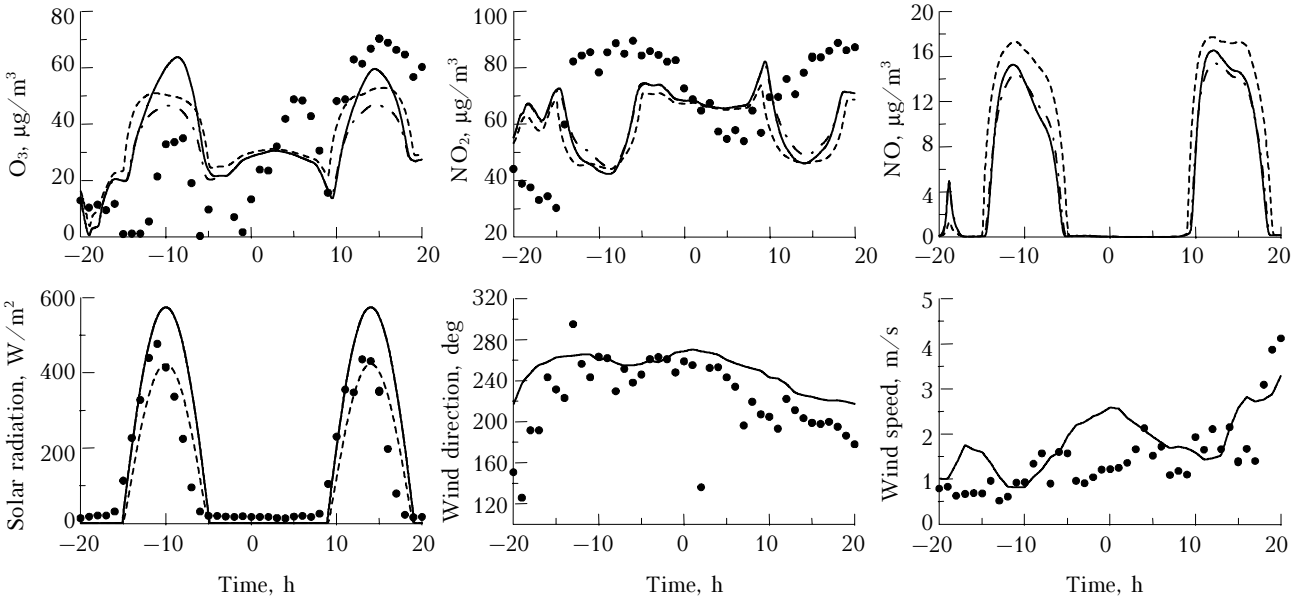

Fig. 4. Comparison of ozone, nitric oxide, and dioxide concentrations; wind speed and direction; solar radiation, calculated by different models and measured on October 15–16, 2003. The following initial background values were used in calculations: 39 μg/m^3 (O_3), 56 μg/m^3 (NO_2), 4.3 μg/m^3 (NO), and 0.1 mg/m^3 (CO). The designations are the same as in Fig. 3.

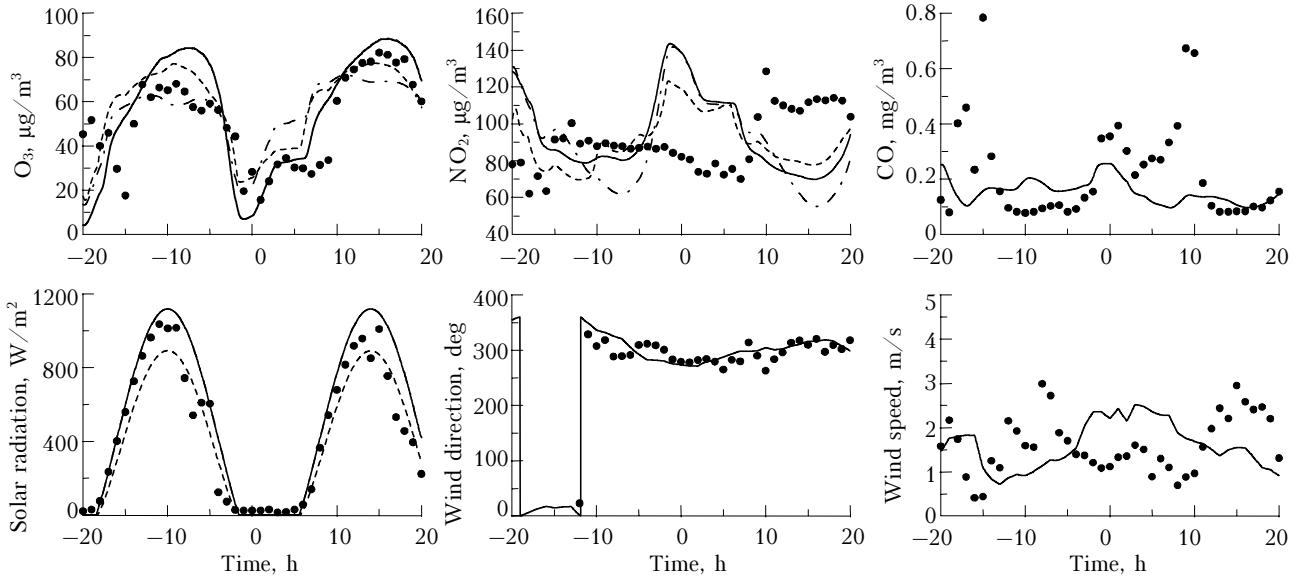

Fig. 5. Comparison of ozone, nitric dioxide and carbon monoxide concentrations; wind speed and direction; and solar radiation, calculated by different models and measured on May 26–27, 2004. The following initial background values were used in calculations: 49 μg/m^3 (O_3), 93.5 μg/m^3 (NO_2), 4.3 μg/m^3 (NO), and 0.1 mg/m^3 (CO). The designations are the same as in Fig. 3.

transport of impurities to the upper atmospheric boundary layer, that stimulates the impurity accumulation near the surface. Morning destruction of inversion due to solar radiation and warming-up of the Earth surface, *vice versa*, intensifies exchange processes between low and upper atmospheres and, hence, stimulates the impurity dispersion.

Thus, the agreement between calculated profiles of O_3 concentrations and measured data confirms a permissibility of application of the described models to studying the formation and dispersion of ground ozone in urban areas. Satisfactory agreement between calculated and observed values of the carbon monoxide ground level concentration points out to the adequacy of representation of advection–diffusion processes in the used numerical model of impurity transport.

The diurnal dynamics of the ground ozone concentration distribution in the domain under study was investigated using one of the three considered models, namely, the Azzi GRS-mechanism.[9]

As was noted above, solar radiation level has a dominant impact on the rate of ozone formation, that

is proved in daily variations of the ozone concentration. Another important factors are the location of emission sources, as well as wind speed and direction. Figures 6 and 7 show isolines of ground ozone concentrations at a height of 10 m at 12 a.m. and 10 p.m. on February 20, 2004.

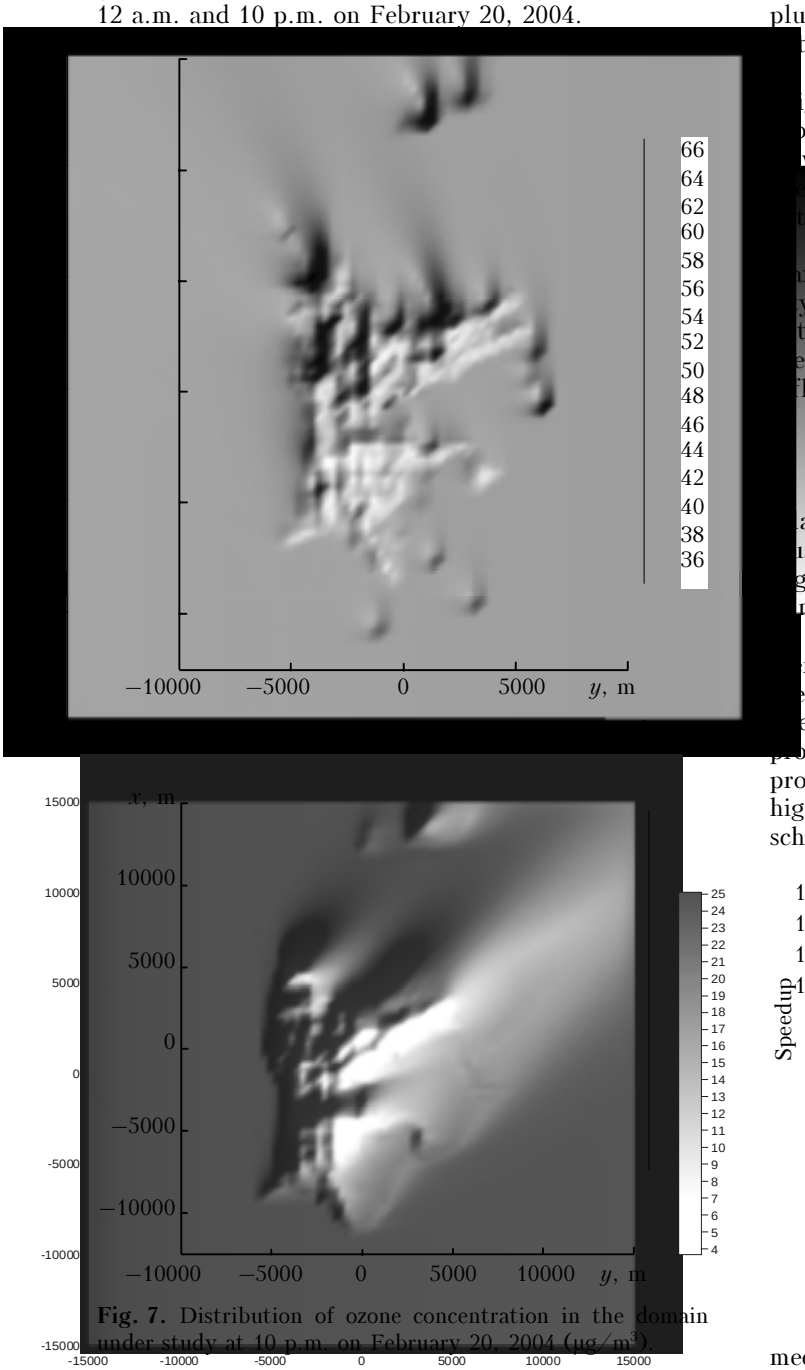

Fig. 7. Distribution of ozone concentration in the domain under study at 10 p.m. on February 20, 2004 (μg/m^3).

During the day hours (Fig. 6), when solar radiation is maximal, minimal values of ground ozone concentration are observed within the city due to high level of nitric monoxide in vehicles and industrial emissions. The range of O_3 maximal concentration is located at the northwest outskirts of the city because of the south-eastern wind, transporting impurity from the city at the time and, hence, creating favorable conditions for ozone generation due to NO_2 photolysis. Besides, industrial enterprises located in the district emit volatile hydrocarbon compounds, the presence of which accelerates the ground ozone formation. Thus, a long plume with an elevated ozone concentration is formed tside the city.

Photochemical reactions cease after the sunset g. 7). Nitric oxide emission leads to almost full one destruction within and outside the city on ward. Therefore, maximal ozone concentrations on windward side of the city, where thropogenic sources influence insignificantly.

Thus, the calculation results show that the ximal ground ozone concentrations are outside the y on leeward during the day hours, that agrees th results of Ref. 16, and on windward outskirts of e city after the sunset, where there is no the city fluence, connected with nitric monoxide emission.

Speedup estimation

Speedup estimation of the parallel algorithm ative to the sequential one was conducted at a ister of IAO SB RAS for the above conditions. gure 8 shows the dependence of the speedup on the mber of processors.

Practically linear growth of performance can be n for small number of processors: at 10 units the eedup amounts to 9 while at 20 units – only to 15 e to IPC overhead. Thus, the use of more than 10 ocessors is less efficient. However, this loss in the program performance is insignificant, that proves a high degree of the algorithm parallelism and a good scheduling of interprocessor communications.

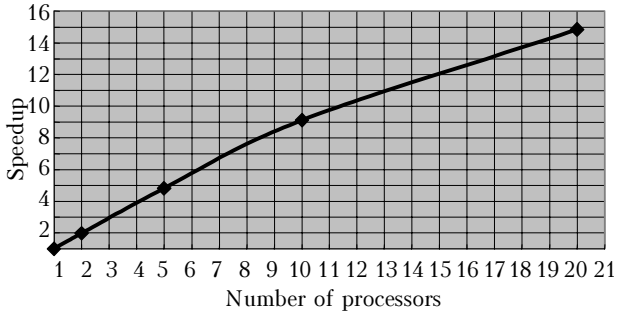

Fig. 8. Speedup of the parallel program.

Conclusion

Comparison of three abridged kinetic mechanisms of ozone formation is presented. Good agreement between calculated and measured ground level concentrations of air pollutants, wind speed and direction proves a possibility of using the considered models for investigation of formation, transformation and dispersion of ozone within and outside the city.

The models allowed us to reveal some features of urban air pollution with ozone and its precursors, to establish factors influencing the formation and destruction of secondary pollutants, to study daily

behavior of spatial distribution of the ground ozone concentration. The models can be used for real-time air quality prediction, because they provide for the high-speed predictions of a high accuracy.

Acknowledgments

This work was financially supported by the Russian Foundation for Basic Research (Grant No. 04-07-90219) and Federal Education Agency (Grant No. A04-2/10-770).

References

1. T.R. Oke, *Climates of Boundary Layer* (Gidrometeoizdat, Leningrad, 1982), 360 pp.
2. N. Moussiopoulos, P. Sahm, and C. Kessler, Atmos. Environ. **29**, No. 24, 3619–3632 (1995).
3. A.V. Starchenko, D.A. Belikov, and A.O. Esaulov, in: *Proc. of ENVIROMIS 2002 Conf.* (Tomsky CNTI, Tomsk, 2002), pp. 142–151.
4. V.V. Penenko and M.G. Korotkov, Atmos. Oceanic Opt. **11**, No. 6, 492–496 (1998).
5. EURAD: http://www.eurad.uni-koeln.de.
6. ADMS-Urban: http://www.cerc.co.uk/software/urban.htm.
7. M. McIven and L. Filips, *Atmospheric Chemistry* (Mir, Moscow, 1978), 375 pp.
8. W.R. Stockwell, F. Kirchner, M. Kuhn, and S. Seefeld, J. Geophys. Res. D **102**, 25847–25879 (1997).
9. P.J. Hurley, *The Air Pollution Model* (TAPM) Version 1: *Technical Description and Examples*. CSIRO Atmospheric Research Technical Paper No. 43 (CSIRO, Aspendale, 1999), 39 pp.
10. R.P. Morison, L.M. Leslie, and M.S. Speer, Meteorol. and Atmos. Phys. **80**, Nos. 1–4, 141–151 (2002).
11. E.V. Korolenok and O.V. Nagornov, Mat. Model. **14**, No. 4, 80–94 (2002).
12. J.H. Seinfeld, *Atmospheric Chemistry and Physics of Air Pollution* (Wiley, New York, 1986), 738 pp.
13. M.E. Berlyand, *Modern Problems of Atmospheric Diffusion and Air Pollution* (Gidrometeoizdat, Leningrad, 1975), 448 pp.
14. A.V. Starchenko and D.A. Belikov, Atmos. Oceanic Opt. **16**, No. 7, 608–615 (2003).
15. S. Perego, Meteorol. and Atmos. Phys. **70**, Nos. 1–2, 43–69 (1999).
16. P. Tulet, A. Maaley, V. Crassier, and R. Rosset, Atmos. Environ. **33**, No. 11, 1651–1662 (1999).